Received 28 June 2021; revised 15 August 2021; accepted 16 September 2021. Date of publication 28 September 2021; date of current version 28 October 2021.
The review of this article was arranged by Editor M. J. Kumar.

Digital Object Identifier 10.1109/JEDS.2021.3116046

A Numerical Approach for Space Charge Limited Bipolar Flow in Cylindrical diodes

MEI YAN LIAO[1,2], RUO HE YAO[1,2], AND YING BIN ZHU[1,2] (Member, IEEE)

1 School of Electronic and Information Engineering, South China University of Technology, Guangzhou 510006, China
2 School of Microelectronics, South China University of Technology, Guangzhou 510006, China

CORRESPONDING AUTHOR: Y. B. ZHU (e-mail: yingbinzhu@outlook.com)

This work was supported in part by the National Natural Science Foundation of China (NSFC) under Grant 61801182; in part by the Fundamental Research Funds for the Central Universities under Grant 2019XX18; and in part by the State Key Laboratory of Optoelectronic Materials and Technologies Open Fund, Sun Yat-sen University under Grant OEMT-2018-KF-07.

ABSTRACT In this paper, a numerical iteration approach to resolve the space charge limited (SCL) bipolar flow problem in cylindrical geometries has been developed. Such an approach is basis for the simultaneous determination of the unknown current densities and the potential distribution. We employed this method to study the characteristics of the SCL bipolar flow. By considering a cylindrical geometry with a cathode radius R_c and an anode radius R_a, the enhancement over the classical Langmuir-Blodgett (LB) law is investigated as a function of R_c/R_a. It is found that for the bipolar flow model, the SCL current density can be given by $F \times J_{LB}$, where F and J_{LB} represent the enhancement factor on account of the influence of ions and the LB law, respectively. The enhancement factor F follows a R_c/R_a scaling and gradually converges to a constant with increasing R_c/R_a. The planar bipolar flow solution is recovered in the condition where the values of R_c and R_a are much greater than that of the gap spacing.

INDEX TERMS Bipolar flow, current density, space-charge-limited (SCL).

I. INTRODUCTION

Space-Charge-Limited (SCL) current flow has received lots of attention in vacuum electronic devices (VEDs), for it has an important effect on the modeling high power microwaves (HPM) and x-ray sources, heavy ion beams, compact high power THz sources, and free electron lasers [1], [2]. Emitted from the cathode, electrons move toward the anode under the control of electric fields, forming a space current. These accumulated charges in the space will give rise to the electric fields that repel charges of the same sign. For a one dimensional (1D) planar geometry, the SCL current density is governed by the well known Child–Langmuir (CL) law [3], [4]

$$J_{CL} = \frac{4}{9}\varepsilon_0\sqrt{\frac{2e}{m}}\frac{V_0^{3/2}}{D^2}, \tag{1}$$

where e and m are the charge and mass of an electron, respectively, and ε_0, V_0, and D are the permittivity of the free space, the gap voltage, and gap spacing of the electrodes, respectively. For different applications, the classical CL law may be inapplicable. Therefore, there are extensions to the CL law to the cylindrical and spherical geometries [5]–[9], multidimensions [10]–[13], quantum regime [14]–[16], relativistic effect [17]–[20], time dependent current injection [21]–[23], and influence of initial velocity [24]–[27]. Moreover, the theories of SCL have been used to make an investigation of some space charge dominated systems, such as THz oscillation [28]–[32], Coulomb blockade [33], bipolar flow [34]–[37], optical field emission at high field [38]–[44], photon-enhanced thermionic energy converters (PETEC) [45], and nanodiodes [46].

For the cylindrical geometry, Langmuir and Blodgett (LB) obtained the SCL current density on the cathode [5],

$$J_{LB} = \frac{4}{9}\varepsilon_0\sqrt{\frac{2e}{m}}\frac{V_0^{3/2}}{R_a R_c \beta^2}, \tag{2}$$

where R_c and R_a are the cathode radius and the anode radius, respectively, and β is a function of R_a/R_c tabulated numerically. But LB solutions are difficult to obtain and rely on complicated series expansions. Chen *et al.* [6] proposed a physical approximation to analyze the SCL current in a cylindrical geometry. In [5], a transit time model is

applied to the cylindrical and spherical geometries and a new scaling laws was found. Harsha and Garner [7] applied conformal mapping to derive the analytical solutions of SCL current for various geometries. For high power applications and thermionic energy converters (TEC), outgassing and thermionic emission typically occur [34], [45]. In [9], an approximate current density scaling expressions for cylindrical bipolar diodes in positive and negative polarity for non-relativistic and relativistic regimes are provided. Such a bipolar flow problem is of fundamental interest since positive ions are commonly used to mitigate the space charge effect [45].

For the SCL bipolar flow problem in the cylindrical model, the exact analytical solutions are not easy to obtain. In this paper, we proposed an iteration approach to numerically investigate the SCL bipolar flow problem in a cylindrical geometry without analytically solving the nonlinear Poisson's equation. By discretely dividing the calculation area of the discharge space into grid points, and by applying the finite difference method and appropriate iteration algorithms, the SCL electron current density can be determined for a given injection ion current density.

II. NUMERICAL APPROACH

In this section, we first describe the model of bipolar flow in a cylindrical diode. To obtain the steady-state solution for the SCL electron and ion flow problem, we employ a numerical approach to solve the nonlinear differential equation in accordance with the boundary condition. We will also present an iteration algorithm to numerically derive the SCL electron current density under different conditions. The approach is made up of two parts. The first part iteratively determines the SCL electron current density for a given injection ion current density or parameter q related to the ratio of the ion current density to the electron current density. In light of the results of the first part, the second part updates the ion current density or parameter q. The details of the algorithms will be described below.

A. MODEL

In the present numerical approach, we make use of the Poisson's equation to numerically investigate the properties of the SCL current flow in cylindrical diodes in the presence of ions, and assume that the system is collisionless. Let us consider a 1D cylindrical diode with electrodes separated by a distance D, where the anode electrostatic potential is V_0 and the cathode grounded. For electrons and ions respectively injected from the cathode and anode with zero initial velocity, the steady-states of the problem are given by the Poisson's equation

$$\frac{d^2V(r)}{dr^2} + \frac{1}{r}\frac{dV(r)}{dr} = -\frac{1}{\varepsilon_0}[\rho_e(r) + \rho_i(r)], \tag{3}$$

where $V(r)$, $\rho_e(r)$, and $\rho_i(r)$ are the electrostatic potential, electron density, and ion density at coordinate r, respectively, and R_c and R_a are the cathode radius and anode radius, respectively. The electron and ion charge densities can be respectively expressed as

$$\rho_e(r) = \frac{R_c J_e}{r|v_e(r)|}, \tag{4}$$

$$\rho_i(r) = -\frac{R_a J_i}{r|v_i(r)|}, \tag{5}$$

where $v_e(r)$ and $v_i(r)$ are respectively the electron and ion velocities at coordinate r, and J_e and J_i denote the electron and ion current densities at the cathode and anode, respectively.

By combining (3) with (4) and (5), and using conservation of energy, we have

$$r\frac{d^2V(r)}{dr^2} + \frac{dV(r)}{dr} = -\frac{R_c J_e}{\varepsilon_0}\left(\frac{m_e}{2e}\right)^{1/2} \times \left\{\frac{1}{V^{1/2}(r)} - \frac{qR_a}{R_c}\frac{1}{[V_0 - V(r)]^{1/2}}\right\}, \tag{6}$$

where the parameter $q = \left(J_i/J_e\right)\left(m_i/Zm_e\right)^{1/2}$ and Z denote the ion charge state. We take proton as example and therefore Z equal to one in this paper. Apparently, $q = 0$ corresponds to no ions or $J_i = 0$ due to $J_e \neq 0$. To numerically obtain the limiting electron current density, we first specify the value of q in (6), but it doesn't mean that there are innumerable solutions. Because a value of q corresponds to unique solutions of J_i and J_e.

The boundary conditions for (6) are given by

$$V(R_c) = 0, V(R_a) = V_0. \tag{7}$$

If the electron and ion current densities are limited, (6) has additional boundary conditions for the zero potential gradient at the cathode and anode given by

$$\left.\frac{dV}{dr}\right|_{r=R_c} = 0, \left.\frac{dV}{dr}\right|_{r=R_a} = 0, \tag{8}$$

It is known that for the 1D bipolar flow model in a planar geometry, the parameter q can be increased from zero to its maximum $q_s = 1$ corresponding to zero potential gradient at the cathode and anode [47]. However, owing to the influence of ions on the system and the nonlinearity in $V(r)$ in the beam, whether the electron and ion current densities can increase to arbitrary values and whether the electrodes can simultaneously satisfy the boundary conditions of (8) are unknown. Moreover, a less obvious impediment to find the solutions of (6) is that the parameter q and electron current density J_e are not specified. For a 1D planar geometry, the range of q and the SCL electron current density can be analytically obtained according to the boundary conditions, but (6) presents formidable analytic difficulties. While it is difficult to solve the nonlinear differential equation of (6) analytically based on the boundary conditions, a numerical approach to analyze the SCL bipolar flow problem is presented.

To numerically solve (6), the calculation area from $r = R_c$ to $r = R_a$ is divided into $N+1$ grid points discretely and

uniformly. Therefore, in the r direction, the spacing of each grid is $h = |R_a - R_c|/N$. Assume that the electrostatic potential of grid point i is V_i, and its corresponding left and right neighboring grid points' electrostatic potential denote as V_{i-1} and V_{i+1}, respectively. Then, performing the second order finite difference and the central difference approaches to the Poisson's equation, we obtain

$$V_i^{n+1} = \frac{1}{2}\left(V_{i+1}^n + V_{i-1}^{n+1}\right) - \frac{h^2}{2} \times \left\{-\frac{V_{i+1}^n - V_{i-1}^{n+1}}{2hr} - \frac{R_c J_e}{r\varepsilon_0}\left(\frac{m_e}{2e}\right)^{1/2} \left[\left(\frac{1}{V_i^n}\right)^{1/2} - \frac{qR_a}{R_c}\frac{1}{\left(V_0 - V_i^n\right)^{1/2}}\right]\right\}, \quad (9)$$

where the superscript n and $n-1$ are denote the n-th and $(n-1)$-th iterative step, respectively. In light of (9), every grid point's electrostatic potential can be updated according to the results, V_i^n, V_{i-1}^n, and V_{i+1}^n, of the last iteration. Hence, by applying appropriate boundary conditions and iteration algorithms, the SCL electron current density can be numerically derived. To speed up the convergence, a relaxation method is introduced into the iteration. Specifically, in calculating the potential of grid point i, the new value of the grid point $i-1$ calculated before is involved. In other words, V_i^{n+1} is calculated by utilizing its left neighboring grid point's new value V_{i-1}^{n+1} instead of the old value V_{i-1}^n, as shown in (9).

B. ITERATION ALGORITHM

In the above analysis, a simple three-point stencil is applied to translate the nonlinear differential equation of (6) into the finite difference form, but the parameter q and electron current density J_e are not specified. Practically, to obtain the potential distribution of the diode, we must first specify the values of q and J_e. After numerically solving for the potential distribution, we can calculate the electric field, defined only at points midway between adjacent grid points, at the electrode. Based on the obtained results, we can further increase J_e until the electric field tends to zero at the cathode. However, as the electron and ion current densities are limited, the electric field varies rapidly near the cathode and anode, which makes the method that manually determines the SCL current densities difficult. In the numerical approach to solve the Poisson's equation, the grid resolution and accurately estimating the true electric field values at the electrodes play an important part in determination of the SCL current density. As the SCL bipolar flow problem in the 1D planar geometry, the parameter q and the limiting electron current density are strongly related to the boundary conditions.

In order to push the electric fields to zero both of the cathode and anode, an iteration approach is presented to update the parameter q and the electron current density J_e consistently. Firstly, two initial electron current densities J_1 and J_2, and an initial value q_1 of the parameter q are given. Considering only the Dirichlet boundary conditions, $V_1 = 0$ and $V_{N+1} = V_0$, we, respectively, solve the restricted nonlinear Poisson's equation to obtain the potential distribution $V(r)$ for the given two sets of initial values, J_1 and q_1, and J_2 and q_1. This process is referred to as inner iteration. After the inner iteration, the corresponding electric field E_c^1 and E_c^2 can be respectively obtained at the cathode. The intermediate iteration predicts a new electron current density J_3, which can be generalized as follows [48]:

$$J^* = -\frac{E_c^{n-1}}{E_c^n - E_c^{n-1}}(J_n - J_{n-1}) + J_{n-1}, \quad (10)$$

$$J_{n+1} = 0.1J^* + 0.9J_n. \quad (11)$$

Note that in the intermediate iteration, an extrapolating function is used to obtain the cathode electric field [48],

$$f(r) = A + Br^{1/3} + Cr^{2/3}, \quad (12)$$

where A is defined as the electric field at the cathode. (12) has three unknown parameters, A, B, and C. Therefore, three nearest half-grid points' electric fields near the cathode are used to fit the extrapolating function. Obviously, the electric field at the cathode is $f(0) = A$, which is used to drive the electric field to zero at the cathode in the intermediate iteration. The intermediate iteration will be terminated, if the value of A is approximately to zero. When the intermediate iteration process is terminated, we can obtain the SCL electron current density and the anode electric field E_a^1 based on (12), with the corresponding value $q = q_1$. Similarly, if a different initial value $q = q_2$ is used, we can obtain the corresponding anode electric field E_a^2. Pushing the anode electric field to zero requires predicting a new parameter q_3 based on the anode electric fields E_a^1 and E_a^2 following a similar iteration process as above, given by

$$q^* = -\frac{E_a^{n-1}}{E_a^n - E_a^{n-1}}(q_n - q_{n-1}) + q_{n-1}, \quad (13)$$

$$q_{n+1} = 0.1q^* + 0.9q_n, \quad (14)$$

where the anode electric fields are calculated by (12). This process is referred to as outermost iteration. It is clear that the SCL bipolar flow problem can be solved by combining the inner, intermediate, and outermost iterations.

To summarize, the numerical approach consists of an inner iteration, an intermediate iteration, and an outermost iteration, as shown in Fig. 1. In the flowchart, the values of a and b are the convergence criterion used in the intermediate and outermost iterations, respectively. Specifically, the inner iteration uses the finite different method to solve the restricted nonlinear Poisson's equation by considering the boundary conditions of (7) for a given parameter q and electron current density J_e. The intermediate iteration utilizes results of the inner iteration to calculate a new electron current density that would push the cathode electric field to zero according to (10) and (11). As the cathode electric field E_c satisfies the convergence criterion, $E_c \leq a$, the

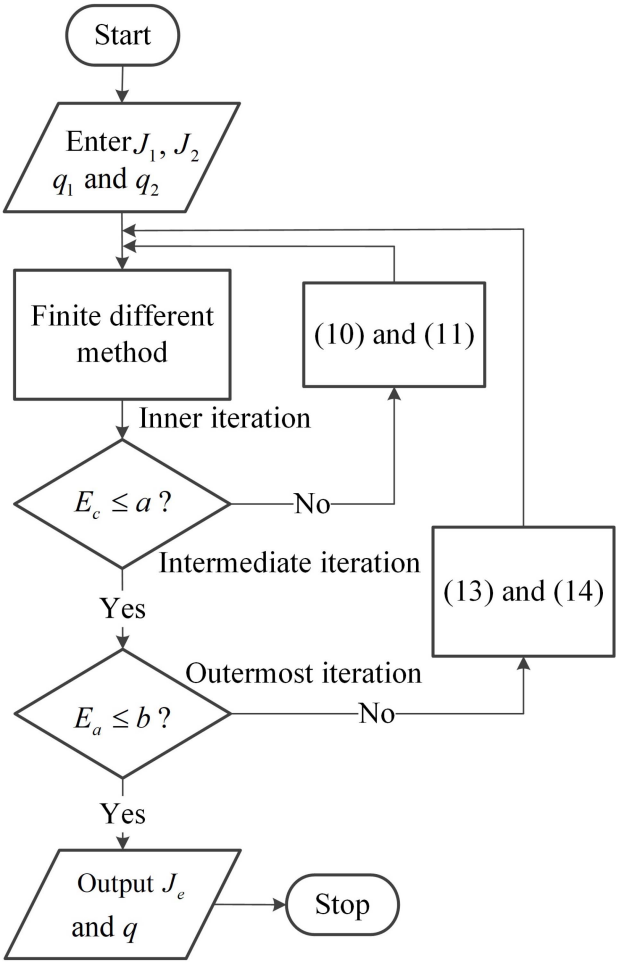

FIGURE 1. The flowchart of the numerical approach.

intermediate iteration process will be terminated. In the outermost iteration, a new value of q is predicted in light of (13) and (14), which would drive the anode electric field to zero. The numerical iteration continues until the anode electric field E_a satisfies the convergence criterion, $E_a \le b$.

Note that if the injection ion current density is given, it is difficult to employ the inner iteration to obtain the SCL electron current density because the initial electron current density is probably so small that the corresponding SCL ion current density is less than the given injection ion current density, leading to the over-injection of the initial ion current density. Therefore, to calculate the SCL electron current density, we specify the parameter q instead of giving the value of the ion current density. After obtaining the SCL electron current density, the corresponding ion current density can be derived in accordance with the value of q.

On the other hand, in [48], a secant method is introduced to evolve the limiting electron current density, with the corresponding zero electric field on the cathode. However, for a given value of q or ion current density, the final anode electric field are probably not zero. Therefore, the secant method may be extended to different anode boundary conditions. Specifically, giving a value of anode electric field, we may employ the extended method to drive the corresponding value of q or ion current density. Assume that the anode electric field is E_{a0} when the electron current density is SCL in the absence of ions. It is known that the anode electric field E_{a0} will be increased if the positive ions are involved, and further increasing the ion current density can drive the anode electric field to zero corresponding to the SCL bipolar flow. Therefore, if we want to obtain the SCL electron current density for an arbitrary value of the anode boundary condition, (13) can be extended to the form

$$q^* = \frac{E_{ba} - E_a^{n-1}}{E_a^n - E_a^{n-1}}(q_n - q_{n-1}) + q_{n-1}, \tag{15}$$

where E_{ba} $(0 \le E_{ba} \le |E_{a0}|)$ denotes the given boundary condition of anode. It is clear that (15) is identical to (13) when $E_{ba} = 0$. Note that the actual electric field in the space is negative, but for simplicity we use the absolute value of the electric field to calculate new values.

III. RESULTS DISCUSSION

In Section II, a numerical iteration approach is proposed to solve for the SCL bipolar flow problem in a cylindrical geometry. In this section, we illustrate the numerical results obtained from the iteration method under different conditions, and study the electron current density enhancement over the cylindrical unipolar flow model as a function of R_c/R_a.

Fig. 2(a) shows the numerical evolution of the normalized injection electron current density J_e and the normalized cathode electric field E_c through the inner and intermediate iterations processes for several values of q, where $E_0 = V_0/D$, and J_{CL} is calculated by (1). As discussed in the previous section, by combining the inner and intermediate iterations, the cathode electric field can be pushed to zero. For a given parameter q, the iteration process starts with two given initial current densities J_1 and J_2, and the corresponding cathode electric fields E_1 and E_2 in steady state are respectively derived through the inner iteration. Then, a new electron current density J_3 is predicted by the intermediate iteration. This iteration process is repeated until the cathode electric field is driven to zero, as shown in Fig. 2(a). Fig. 2(b) plots the corresponding normalized electric field distribution in the diode with the iteration progress for $q = 0.8$, where the electric fields at the cathode and anode surface are calculated by (12). From the figure, we can observe that the electric fields near the cathode vary rapidly when the electron current density is approximately SCL. Therefore, it is difficult to accurately determine the SCL current densities by the manual method.

With the iteration progress, the numerical evolution of the parameter q and the normalized anode electric field, and the corresponding normalized electric field distribution in the diode are plotted in Figs. 3(a) and (b), respectively. As shown in Fig. 3(a), the two initial values q_1 and q_2 are respectively

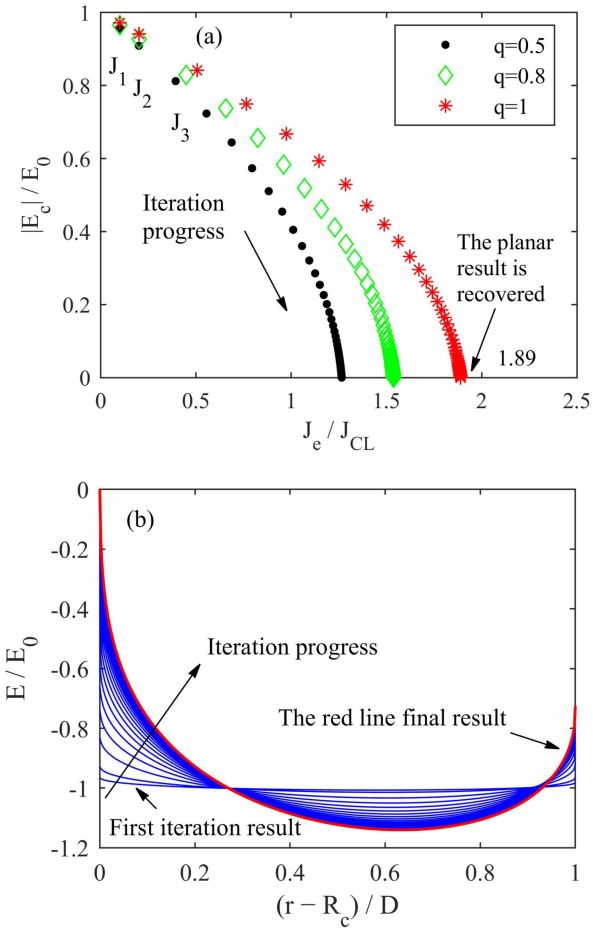

FIGURE 2. **(a) The numerical evolution of the normalized injection electron current density and the normalized cathode electric field with the iteration progress for several values of q and (b) the corresponding numerical evolution of the normalized electric field distribution in the diode for $q = 0.8$, where $V_0 = 1$ V, $R_c = 1$ cm, $D = 0.01$ mm, and $R_c < R_a$. The red line denotes the final iteration result.**

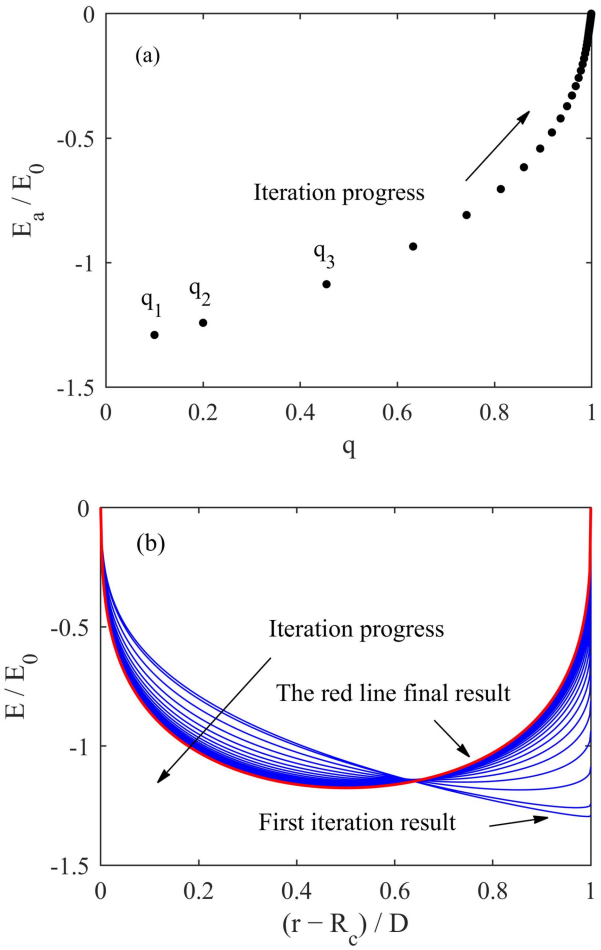

FIGURE 3. **(a) The numerical evolution of the parameter q and the normalized node electric field with the iterative progress, and (b) the corresponding numerical evolution of the normalized electric field distribution in the diode, where $V_0 = 1$ V, $R_c = 1$ cm, $D = 0.01$ mm, and $R_c < R_a$. The red line denotes the final iteration result.**

used to derive the anode electric field. Note that the value of the electric field E_a in Fig. 2(a) corresponds to the steady state that the electron current density is SCL. Therefore, for a given value of q, the anode electric field E_a can be obtained by the inner and intermediate iterations processes, as shown in Fig. 2. After the convergence criterion is reached in the intermediate iteration, (12) is employed to calculate the anode electric field E_a based on the electric field distribution in the diode. According to the first iteration and the second iteration results, a new value q_3 is predicted by the outermost iteration. These processes will not be terminated until the outermost iteration converges, as shown in Fig. 3(a). On the other hand, in Fig. 3(b), every curve represents the electric field distribution in a steady-state that electron current density is SCL. From the figure, it is clear that the value of the first point of every curve is approximately zero, and the anode electric field is pushed to zero with the iteration progress. When the outermost iteration is terminated, the ion and electron current densities are SCL.

Fig. 4 plots the SCL electron current density J_e scaled by the LB law as a function of the cathode radius R_c or the anode radius R_a for several values of q. J_{LB} is analytically calculated by (8) in [5]. Note that the variable R shown in Fig. 4 denotes the cathode radius R_c for the solid lines, and represents the cathode radius R_a for the dash-dot lines. Fig. 4 shows that J_e increases with increasing q for a given radius. It means that positive ions introduced into the discharge space can enhance the SCL electron current density. Moreover, J_e gradually converges to the planar result with increasing cathode or anode radius. In addition, for $R_c < R_a$ and q fixed, the normalized SCL electron current density is also higher than the result for the planar ion diode. The differences will be enhanced with increasing the parameter q. By contrast, for $R_c > R_a$ and q fixed, the normalized SCL electron current density is always less than the result for the planar ion diode as R is relatively small. This is because for $R_c > R_a$ the ion current density monotonically decreases from the anode to the cathode while the ion current density is a constant for the planar geometry, leading to the limiting

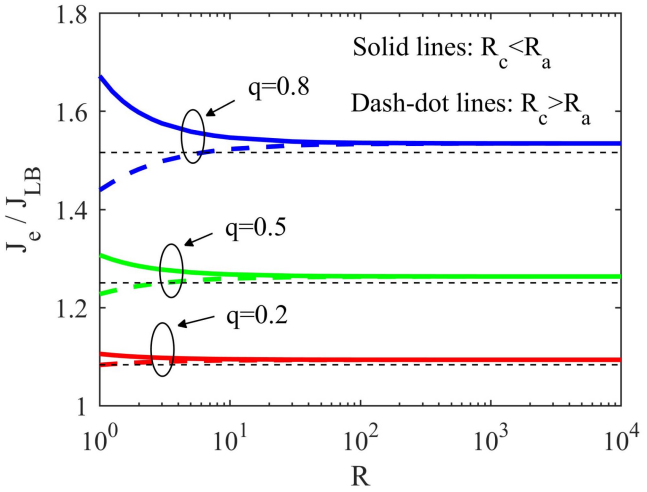

FIGURE 4. Variation of the normalized SCL electron current density J_e with the cathode radius R_c or the anode radius R_a for gap spacing fixed and several values of q. The black dot lines show the theory results normalized to J_{CL} for the planer ion diode, the dash-dot lines show the numerical results with R_a for R_c fixed and $R_c > R_a$, and the solid lines show the numerical results with R_c for R_a fixed and $R_c < R_a$. The anode-cathode spacing is a constant, $D = 0.1$ cm.

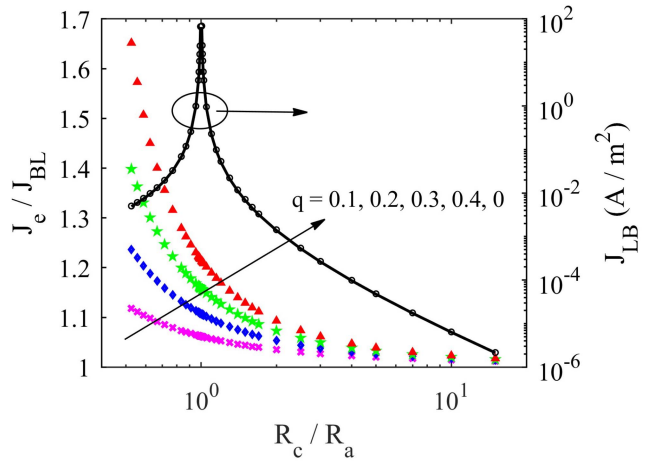

FIGURE 5. Comparison between the LB law (black solid line) and the bipolar flow results scaled by the LB law with R_c/R_a for several values of q, where the black circle show the numerical results of the LB law. The inner radius either R_c or R_a is 1 cm. The applied voltage is 100 V. Symbols: crosses, diamonds, stars, and triangles represent the numerical results scaled by the LB law for $q = 0.1, 0.2, 0.3, 0.4$, respectively.

electron current density for the cylindrical geometry smaller than that of the planar geometry, and vice versa.

Fig. 5 shows the LB solutions and bipolar flow results scaled by the LB law with the ratio of the cathode radius R_c to the anode radius R_a for several values of q. The black solid line stands for the LB solutions analytically obtained by (8) in [5]. From the figure, it is clear that the numerical results corresponding to the solid circles are in agreement with the analytical results, which verifies the correctness of our method. From the curves, we can observe that the normalized SCL current density gradually increases with the decreasing of R_c/R_a. This is because when $R_c < R_a$, the ion

TABLE 1. Fitting results for several values of q.

q	a_1	a_2	a_3	a_4	Γ
0.1	−0.0579	0.0354	−0.0123	0.0017	1.062
0.2	−0.1241	0.0888	−0.0351	0.0054	1.107
0.3	−0.2114	0.1763	−0.0789	0.0128	1.158
0.4	−0.3359	0.3392	−0.1692	0.0296	1.214
0.5	−0.4156	0.4232	−0.5783	0.6862	1.281
0.6	−0.5825	0.7366	−1.2720	1.4840	1.357

current density monotonically increases from the anode to the cathode, leading to a higher electron current that allows to transport across the space, and vice versa.

In light of the numerical results shown in Fig. 5, the SCL electron current density for the bipolar flow model in the cylindrical diode can be written in a general form,

$$J_{bipolar} = F \times J_{LB}, \tag{16}$$

where F is an enhancement factor depending on the parameter q and the ratio of R_c to R_a. The enhancement factor F can be fitted by

$$F = \sum_{n=1}^{M} (-1)^n a_n \left[\ln\left(\frac{R_c}{R_a}\right) \right]^n + \Gamma, \tag{17}$$

where M is an integer greater than one, and the forms of a_n and Γ can be determined according to the numerical results. For $M = 4$, the Table 1 gives the fitting results of a_n and Γ for several values of q by the fitting function. The parameters a_1, a_2, a_3, and a_4 can be respectively summarized with the power functions of q,

$$a_1 = -1.161q^{1.396}, \tag{18a}$$
$$a_2 = 2q^{2.035}, \tag{18b}$$
$$a_3 = -12.77q^{4.511}, \tag{18c}$$
$$a_4 = 22.19q^{5.264}. \tag{18d}$$

While the parameter Γ can be fitted by the linear function of q,

$$\Gamma = 0.5663q + 1. \tag{19}$$

Obviously, for (16) the classical LB solution is recovered when $q = 0$. For (18a)–(18d) and (19), the R-square are 0.994, 0.981, 0.997, 0.981, and 0.989, respectively.

It is known that the anode electric field will be increased if the ions are introduced into the space, as shown in Fig. 6. Therefore, the secant method [48] can be extended to different boundary conditions. Fig. 6(a) plots a comparison of the SCL electron current density derived by the inner iteration and the intermediate iteration processes with those obtained by the extended secant method. The dash line shows the corresponding anode electric field as the electron current density is SCL. We select five values of anode electric field which is used in the extended secant method. Obviously, the results of the two methods are consistent. For a given anode boundary condition $E_a/E_0 = -0.96$ corresponding to $q = 0.6$, Fig. 6(b) illustrates the numerical evolution of the

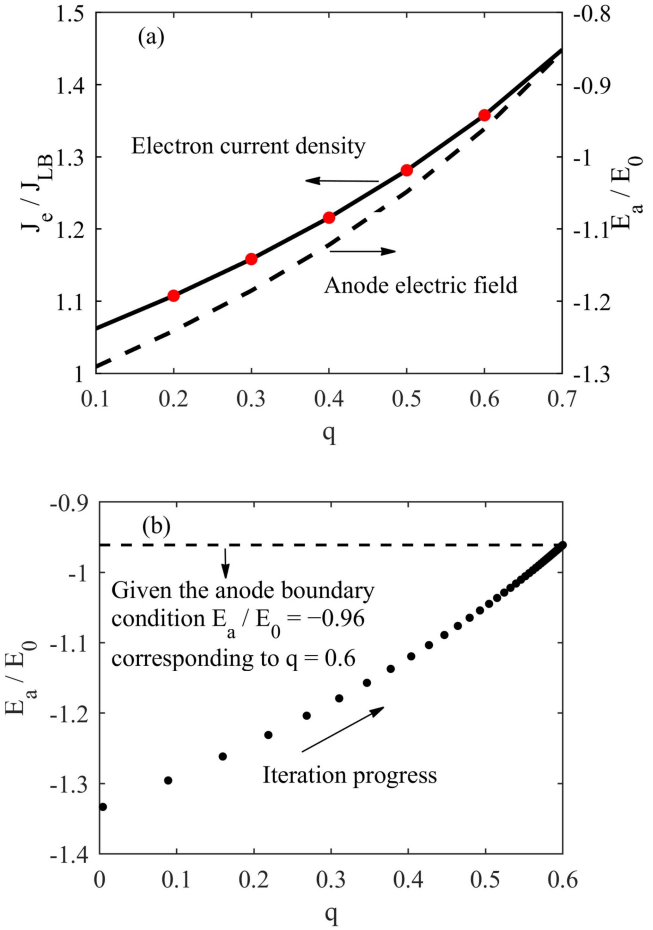

FIGURE 6. **(a) The numerical results of the normalized SCL electron current density and the corresponding normalized anode electric field with the parameter *q*, where the red dots show the results obtained by the extended secant method, and (b) the numerical evolution of the normalized anode electric field with the iteration progress for a given anode boundary condition.**

anode electric field with the iteration progress. It is clear that the final result converges to $q = 0.6$ identical to the result shown in Fig. 6(a).

In order to more clearly illustrate the important effect of positive ions, we plot the comparison between the spatial profiles in the presence of ions and the spatial profiles in the absence of ions, as shown in Fig. 7. In the numerical calculation, all of the results in Fig. 7(a) are obtained by employing the inner iteration method as mentioned above. From the Fig. 7(a), we can observe that with increasing the parameter q, the curves become steeper and increase slowly near the anode region, indicating that potential gradients at the anode tend to zero as the parameter q increases. The field distribution curves shown in Fig. 7(b) validates the numerical results of $V(r)$. Obviously, as q increases to its maximum value of one, the electric fields at the cathode and the anode are approximately zero, representing the SCL bipolar flow.

On the other hand, the ratio of electron density ρ_e to ion density ρ_i monotonically decreases from cathode to anode

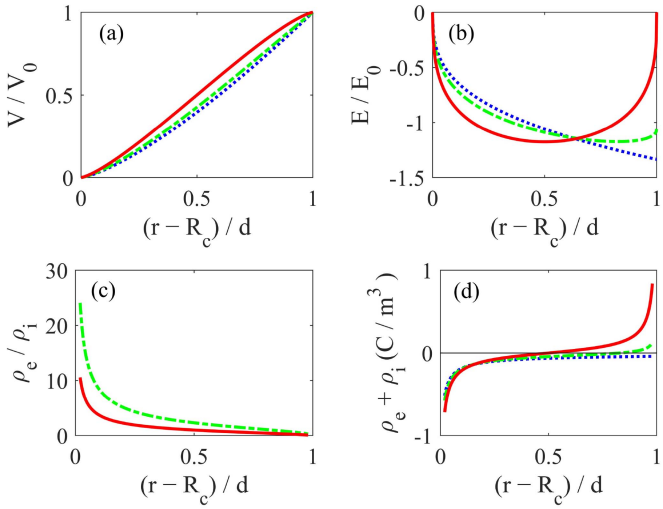

FIGURE 7. **Spatial profiles of (a) the normalized potential, (b) the normalized electric field, (c) the local ratio of electron density ρ_e to ion density ρ_i, and (d) the local charge density, where the blue dot lines, the green dash-dot lines, and the red solid lines show the numerical results with $q = 0$, $q = 0.5$, and $q = 1$, respectively.**

shown in Fig. 7(c). Moreover, as shown in Fig. 7(d), positive ions introduced into the discharge can substantially neutralize the charge density, and the charge neutral point r_n, corresponding to $\rho_e(r_n) + \rho_i(r_n) = 0$, shifts towards the cathode as the parameter q increases. Note that the neutral point r_n is the location where the electric field is zero. In addition, when $q = 1$, the total charge density from cathode to anode is approximately zero, leading to zero potential gradient at the electrodes.

IV. CONCLUSION

In summary, a numerical iteration approach has been proposed to investigate the SCL bipolar flow problem in a cylindrical geometry. Utilizing the approach without analytically solving the Poisson equation, we could easily simultaneously determinate the unknown current densities and the potential distribution, and derive the SCL electron current density under different conditions. Calculations show that for the bipolar model in the cylindrical geometry, it can exceed the classical LB law given by $F \times J_{LB}$. The enhancement factor F follows a R_c / R_a scaling and would converge to a constant as the value of R_c / R_a are large enough. We also extend the secant method to different boundary conditions, and simulation shows that the results of the two methods are consistent.

REFERENCES

[1] P. Zhang, A. Valfells, L. K. Ang, J. W. Luginsland, and Y. Y. Lau, "100 years of the physics of diodes," *Appl. Phys. Rev.*, vol. 4, no. 1, Mar. 2017, Art. no. 011303, doi: 10.1063/1.4978231.

[2] P. Zhang, Y. S. Ang, A. L. Garner, A. Valfells, J. W. Luginsland, and L. K. Ang, "Space–charge limited current in nanodiodes: Ballistic, collisional, and dynamical effects," *J. Appl. Phys.*, vol. 129, no. 10, Mar. 2021, Art. no. 100902, doi: 10.1063/5.0042355.

[3] C. D. Child, "Discharge from hot CaO," *Phys. Rev.*, vol. 32, no. 5, pp. 492–511, May 1911, doi: 10.1103/PhysRevSeriesI.32.492.

[4] I. Langmuir, "The effect of space charge and residual gases on thermionic currents in high vacuum," *Phys. Rev.*, vol. 2, no. 6, pp. 450–486, Dec. 1913, doi: 10.1103/PhysRev.2.450.
[5] Y. B. Zhu, P. Zhang, A. Valfells, L. K. Ang, and Y. Y. Lau, "Novel scaling laws for the Langmuir-Blodgett solutions in cylindrical and spherical diodes," *Phys. Rev. Lett.*, vol. 110, no. 26, Jun. 2013, Art. no. 265007, doi: 10.1103/PhysRevLett.110.265007.
[6] X. P. Chen, J. Dickens, L. L. Hatfield, E.-H. Choi, and M. Kristiansen, "Approximate analytical solutions for the space-charge-limited current in one-dimensional and two-dimensional cylindrical diodes," *Phys. Plasmas*, vol. 11, no. 6, p. 3278, Apr. 2004, doi: 10.1063/1.1743309.
[7] N. R. S. Harsha and A. L. Garner, "Applying conformal mapping to derive analytical solutions of space-charge-limited current density for various geometries," *IEEE Trans. Electron Devices*, vol. 68, no. 1, pp. 264–270, Jan. 2021, doi: 10.1109/TED.2020.3038619.
[8] A. M. Darr and A. L. Garner, "A coordinate system invariant formulation for space-charge limited current in vacuum," *Appl. Phys. Lett.*, vol. 115, no. 5, Jul. 2019, Art. no. 054101, doi: 10.1063/1.5115261.
[9] I. M. Rittersdorf, P. F. Ottinger, R. J. Allen, and J. W. Schumer, "Current density scaling expressions for a bipolar space-charge-limited cylindrical diode," *IEEE Trans. Plasma Sci*, vol. 43, no. 10, pp. 3626–3636, Oct. 2015, doi: 10.1109/TPS.2015.2471275.
[10] J. W. Luginsland, Y. Y. Lau, and R. M. Gilgenbach, "Two-dimensional Child-Langmuir law," *Phys. Rev. Lett.*, vol. 77, no. 22, pp. 4668–4670, Nov. 1996, doi: 10.1103/PhysRevLett.77.4668.
[11] Y. Y. Lau, "Simple theory for the two-dimensional Child-Langmuir law," *Phys. Rev. Lett.*, vol. 87, no. 27, Dec. 2001, Art. no. 278301, doi: 10.1103/PhysRevLett.87.278301.
[12] W. S. Koh, L. K. Ang, and T. J. T. Kwan, "Multidimensional short-pulse space-charge-limited flow," *Phys. Plasmas*, vol. 13, no. 6, May 2006, Art. no. 63102, doi: 10.1063/1.2208086.
[13] M. Zubair and L. K. Ang, "Fractional-dimensional Child-Langmuir law for rough cathode," *Phys. Plasmas*, vol. 23, no. 7, Jun. 2016, Art. no. 072118, doi: 10.1063/1.4958944.
[14] Y. Y. Lau, D. Chernin, D. G. Colombant, and P.-T. Ho, "Quantum extension of Child-Langmuir law," *Phys. Rev. Lett.*, vol. 66, no. 11, pp. 1446–1449, Mar. 1991, doi: 10.1103/PhysRevLett.66.1446.
[15] L. K. Ang, T. J. T. Kwan, and Y. Y. Lau, "New scaling of Child-Langmuir law in the quantum regime," *Phys. Rev. Lett.*, vol. 91, no. 20, Nov. 2003, Art. no. 208303, doi: 10.1103/PhysRevLett.66.1446.
[16] S. Bhattacharjeea, A. Vartak, and V. Mukherjee, "Experimental study of space-charge-limited flows in a nanogap," *Appl. Phys. Lett.*, vol. 92, no. 19, Apr. 2008, Art. no. 191503, doi: 10.1063/1.2928232.
[17] J. W. Poukey, "Ion effects in relativistic diodes," *Appl. Phys. Lett.*, vol. 26, no. 4, pp. 145–146, Sep. 1975, doi: 10.1063/1.88121.
[18] C. Litwin and R. Rosner, "Relativistic space-charge-limited bipolar flow," *Phys. Rev. E, Stat. Phys. Plasmas Fluids Relat. Interdiscip. Top.*, vol. 58, no. 1, pp. 1163–1164, Jul. 1998, doi: 10.1103/PhysRevE.58.1163.
[19] L. K. Ang and P. Zhang, "Ultrashort-pulse Child-Langmuir law in the quantum and relativistic regimes," *Phys. Rev. Lett.*, vol. 98, no. 16, Apr. 2007, Art. no. 164802, doi: 10.1103/PhysRevLett.98.164802.
[20] A. D. Greenwood, J. F. Hammond, P. Zhang, and Y. Y. Lau, "On relativistic space charge limited current in planar, cylindrical, and spherical diodes," *Phys. Plasmas*, vol. 23, no. 7, Jun. 2016, Art. no. 072101, doi: 10.1063/1.4954827.
[21] M. E. Griswold and N. J. Fisch, "Maximum time-dependent space-charge limited diode currents," *Phys. Plasmas*, vol. 23, no. 1, Jan. 2016, Art. no. 014502, doi: 10.1063/1.4939607.
[22] M. E. Griswold, N. J. Fisch, and J. S. Wurtele, "Amended conjecture on an upper bound to time-dependent space-charge limited current," *Phys. Plasmas*, vol. 19, no. 2, Feb. 2012, Art. no. 024502, doi: 10.1063/1.3671961.
[23] M. E. Griswold, N. J. Fisch, and J. S. Wurtele, "An upper bound to time-averaged space-charge limited diode currents," *Phys. Plasmas*, vol. 17, no. 11, Nov. 2010, Art. no. 114503, doi: 10.1063/1.3503661.
[24] P. V. Akimov, H. Schamel, H. Kolinsky, A. Y. Ender, and V. I. Kuznetsov, "The true nature of space-charge-limited currents in electron vacuum diodes: A Lagrangian revision with corrections," *Phys. Plasmas*, vol. 8, no. 8, pp. 3788–3798, Jul. 2001, doi: 10.1063/1.1383287.
[25] R. R. Puri, D. Biswas, and R. Kumar, "Generalization of the Child-Langmuir law for nonzero injection velocities in a planar diode," *Phys. Plasmas*, vol. 11, no. 3, pp. 1178–1186, Feb. 2004, doi: 10.1063/1.1644583.
[26] Y. Feng and J. P. Verboncoeur, "Consistent solution for space-charge-limited current in the relativistic regime for monoenergetic initial velocities," *Phys. Plasmas*, vol. 15, no. 11, Nov. 2008, Art. no. 112101, doi: 10.1063/1.3003071.
[27] T. Lafleur, "Space-charge limited current with a finite injection velocity revisited," *Plasma Sources Sci. Technol.*, vol. 29, no. 6, Jun. 2020, Art. no. 065002, doi: 10.1088/1361-6595/ab9069.
[28] M. Ilkov, K. Torfason, A. Manolescu, and Á. Valfells, "Synchronization in arrays of vacuum microdiodes," *IEEE Trans. Electron Devices*, vol. 62, no. 1, pp. 200–206, Jan. 2015, doi: 10.1109/TED.2014.2370680.
[29] A. Pedersen, A. Manolescu, and Á. Valfells, "Space-charge modulation in vacuum microdiodes at THz frequencies," *Phys. Rev. Lett.*, vol. 104, no. 17, Apr. 2010, Art. no. 175002, doi: 10.1103/PhysRevLett.104.175002.
[30] M. Ilkov, K. Torfason, A. Manolescu, and A. Valfells, "Terahertz pulsed photogenerated current in microdiodes at room temperature," *Appl. Phys. Lett.*, vol. 107, no. 20, Nov. 2015, Art. no. 203508, doi: 10.1063/1.4936176.
[31] M. Siman-Tov, J. G. Leopold, and Y. E. Krasik, "Self-oscillations in an over-injected electron diode—Experiment and analysis," *Phys. Plasmas*, vol. 26, no. 3, Mar. 2019, Art. no. 033113, doi: 10.1063/1.5087708.
[32] M. Siman-Tova, J. G. Leopold, and Y. E. Krasik, "A self-oscillating electron beam experiment," *Phys. Plasmas*, vol. 27, no. 2, Feb. 2020, Art. no. 023104, doi: 10.1063/1.5140037.
[33] Y. B. Zhu and L. K. Ang, "Child-Langmuir law in the Coulomb blockade regime," *Appl. Phys. Lett.*, vol. 98, no. 5, Jan. 2011, Art. no. 051502, doi: 10.1063/1.3549868.
[34] W. S. Koh, L. K. Ang, and S. P. Lau, "Space-charge-limited bipolar flow in a nano-gap," *Appl. Phys. Lett.*, vol. 87, no. 19, Nov. 2005, Art. no. 193112, doi: 10.1063/1.2130526.
[35] A. Smirnova, Y. Raitses, and N. J. Fisch, "Maximizing ion current by space-charge neutralization using negative ions and dust particles," *Phys. Plasmas*, vol. 12, no. 5, May 2005, Art. no. 053503, doi: 10.1063/1.1897715.
[36] M. C. Lin, P. S. Lu, P. C. Chang, B. R. Kelley, and J. P. Verboncoeur, "A relativistic self-consistent model for studying enhancement of space charge limited field emission due to counter-streaming ions," *Phys. Plasmas*, vol. 21, no. 2, Feb. 2014, Art. no. 023118, doi: 10.1063/1.4866601.
[37] B. Ragan-Kelle, J. P. Verboncoeur, and M.-C. Lin, "Optimizing physical parameters in 1-D particle-in-cell simulations with Python," *Comput. Phys. Commun.*, vol. 185, no. 10, pp. 2487–2494, Oct. 2014, doi: 10.1016/j.cpc.2014.05.025.
[38] K. L. Jensen, J. Lebowitz, Y. Y. Lau, and J. Luginsland, "Space charge and quantum effects on electron emission," *J. Appl. Phys.*, vol. 111, no. 5, Mar. 2012, Art. no. 054917, doi: 10.1063/1.3692577.
[39] K. L. Jensen *et al.*, "Discrete space charge affected field emission: Flat and hemisphere emitters," *J. Appl. Phys.*, vol. 117, no. 9, May 2015, Art. no. 194902, doi: 10.1063/1.4921186.
[40] S. Sun and L. K. Ang, "Onset of space charge limited current for field emission from a single sharp tip," *Phys. Plasmas*, vol. 19, no. 3, Mar. 2012, Art. no. 033107, doi: 10.1063/1.3695090.
[41] A. M. Darr, A. M. Loveless, and A. L. Garner, "Unification of field emission and space charge limited emission with collisions," *Appl. Phys. Lett.*, vol. 114, no. 1, Jan. 2019, Art. no. 014103, doi: 10.1063/1.5066236.
[42] A. M. Darr, C. R. Darr, and A. L. Garner, "Theoretical assessment of transitions across thermionic, field, and space-charge-limited emission," *Phys. Rev. Research*, vol. 2, no. 3, Jul. 2020, Art. no. 033137, doi: 10.1103/PhysRevResearch.2.033137.
[43] P. H. Stoltz, J. W. Luginsland, A. Chap, D. N. Smithe, and J. R. Cary, "A new simple algorithm for space charge limited emission," *Phys. Plasmas*, vol. 27, no. 9, Sep. 2020, Art. no. 093103, doi: 10.1063/5.0020781.
[44] S. D. Dynako, A. M. Darr, and A. L. Garner, "Incorporating resistance into the transition from field emission to space charge limited emission with collisions," *IEEE J. Electron Devices Soc.*, vol. 6, pp. 650–654, 2019, doi: 10.1109/JEDS.2019.2920856.
[45] K. A. A. Khalid, T. J. Leong, and K. Mohamed, "Review on thermionic energy converters," *IEEE Trans. Electron Devices*, vol. 63, no. 6, pp. 2231–2241, Jun. 2016, doi: 10.1109/TED.2016.2556751.
[46] J. B. Gunnarsson, K. Torfason, A. Manolescu, and Á. Valfells, "Space-charge limited current from a finite emitter in nano- and microdiodes," *IEEE Trans. Electron Devices*, vol. 68, no. 1, pp. 342–346, Jan. 2021, doi: 10.1109/TED.2020.3037280.
[47] I. Langmuir, "The interaction of electron and positive ion space charges in cathode sheaths," *Phys. Rev.*, vol. 33, no. 6, pp. 954–989, Jun. 1929, doi: 10.1103/PhysRev.33.954.
[48] J. J. Watrous, J. W. Luginsland, and M. H. Frese, "Current and current density of a finite-width, space-charge-limited electron beam in two-dimensional, parallel-plate geometry," *Phys. Plasmas*, vol. 8, no. 9, pp. 4202–4210, Aug. 2001, doi: 10.1063/1.1391262.